

Lepton-Flavor-Violating ALPs at the Electron-Ion Collider: A Golden Opportunity

Hooman Davoudiasl^{*},¹ Roman Marcarelli[†],² and Ethan T. Neil^{‡2}

¹High Energy Theory Group, Physics Department Brookhaven National Laboratory, Upton, NY 11973, USA

²Department of Physics, University of Colorado, Boulder, Colorado 80309, USA

Axion-like particles (ALPs) arise in a variety of theoretical contexts and can, in general, mediate flavor violating interactions and parity non-conservation. We consider lepton flavor violating ALPs with GeV scale or larger masses which may, for example, arise in composite dark sector models. We show that a future Electron-Ion Collider (EIC) can uncover or constrain such ALPs via processes of the type $e A_Z \rightarrow \tau A_Z a$, where A_Z is a nucleus of charge Z and a is an ALP, over a significant part of the relevant parameter space. The production of the ALP can have a large Z^2 enhancement from low Q^2 electromagnetic scattering of the electron from a heavy ion. Using the gold nucleus ($Z = 79$) as an example, we show that the EIC can explore $e - \tau$ flavor violation, mediated by GeV-scale ALPs, well beyond current limits. We also discuss how the EIC electron beam polarization can provide a powerful tool for investigating parity violating ALPs.

INTRODUCTION

Global symmetries arise in a variety of theoretical settings and their spontaneous breaking generally leads to axion-like particles (ALPs) [1–4]. Often the global symmetry is not exact and its small explicit breaking leads to the appearance of relatively light ALPs. In the Standard Model (SM), the spontaneous breaking of chiral symmetries gives rise to pseudo-Nambu-Goldstone bosons, *i.e.* the parity-odd pions, which have axion-like properties. The small masses of light quarks, compared to typical hadronic scale $\Lambda_{\text{QCD}} \sim 200$ MeV, provide explicit chiral symmetry breaking, leading to relatively small pion masses.

One may expect similar phenomena to arise in new sectors of physics, which could provide answers for open questions like the nature of dark matter (DM), for example. New physics sectors at scales of $\mathcal{O}(\text{GeV})$ or less have been considered as potential alternatives to beyond SM (BSM) models at or above the weak scale ~ 100 GeV. In particular, “dark sectors” that could include DM and other related states and interactions have been extensively studied over the last several years. In these setups, new experimental possibilities for discovery of BSM phenomena open up. Due to the relatively low scale and feeble couplings associated with such “dark sectors,” intense sources can provide good prospects for uncovering them.

An example of the aforementioned ideas was proposed in Ref. [5], where a dark $SU(3)$ gauge sector and dark fermions were postulated to explain neutrino masses and DM. That model gives rise to GeV scale ALPs, where a symmetry can provide stability for some of those states, hence allowing them to be DM candidates. The model

can naturally lead to lepton flavor violation (LFV) mediated by ALPs, as well as the emergence of parity violating phenomena in their interactions with the SM leptons. The GeV mass scale for ALPs was studied in the lepton flavor violating but parity preserving limit in Ref. [6]. However, one could generally assume that parity violation is present in the low energy effective field theory (EFT) describing the interactions of ALPs with the SM; we will consider this more general case here.

Motivated by the above considerations, in this work, we examine the possibility of probing ALPs arising at or above the GeV scale, perhaps as part of a new dark sector of physics, at the future Electron-Ion Collider (EIC). Collisions with heavy ions provide a significant coherent enhancement to electromagnetic scattering processes, increasing the production rate for ALPs at the EIC by orders of magnitude compared to the case of electron-proton scattering.

We will study the corresponding EFT assuming LFV and allowing for parity non-conservation [5]. We will show that the projected capabilities of the EIC allow for interesting probes of ALP production in processes that involve LFV, where the emission of the ALP a from the electron beam mediates a transition to a tau lepton: $e \rightarrow \tau a$; here e or τ is an off-shell state. If the final state a can decay inside the detector, as is typically the case in the scenario we consider, we can generally expect further leptonic final states which provide clean detection prospects. If the ALP escapes as missing energy due to decay into invisible final states, the apparent $e \rightarrow \tau$ signal is still highly distinct. In the presence of LFV, non-conservation of parity can have a significant rate, and hence the electron beam polarization can be used to uncover such effects, as we will demonstrate in this work. Our analysis shows that the EIC provides significant capabilities for investigation of ALPs, in theoretically interesting regions of parameter space.

Other works that consider exploring LFV using electron beam facilities include Ref. [7] (EIC) and Ref. [8] (CEBAF), where a leptoquark sector is generally as

^{*}email: hooman@bnl.gov

[†]email: roman.marcarelli@colorado.edu

[‡]email: ethan.neil@colorado.edu

sumed to mediate the effects studied therein. Recent work [9] has also studied the prospects for detecting ALPs through their photon coupling at the EIC.

ALP EFFECTIVE FIELD THEORY

The flavor-violating ALP effective Lagrangian we will adopt for this analysis has been previously considered in Refs. [10–17]. It is given by

$$\mathcal{L} = \frac{1}{2}(\partial_\mu a)^2 - \frac{1}{2}m_a^2 a^2 + \mathcal{L}_\ell + \dots + h.c. \quad (1)$$

where we will be focusing on the term

$$\mathcal{L}_\ell = \frac{\partial_\mu a}{\Lambda} \sum_{\ell\ell'} \bar{\ell} \gamma^\mu (V_{\ell\ell'} + A_{\ell\ell'} \gamma_5) \ell' + h.c. \quad (2)$$

Here, we will take $V_{\ell\ell'}$ and $A_{\ell\ell'}$ to be real, so that the Lagrangian is CP-even. However, note that the presence of the vector-like $V_{\ell\ell'}$ term implies that parity violation is present in general. The parity violation can be parametrized by an angle $\theta_{\ell\ell'}$ by defining $\theta_{\ell\ell'} = -\tan^{-1}(V_{\ell\ell'}/A_{\ell\ell'})$ and $C_{\ell\ell'} = \sqrt{V_{\ell\ell'}^2 + A_{\ell\ell'}^2}$, so that

$$\mathcal{L}_\ell = \frac{C_{\ell\ell'}}{\Lambda} \partial_\mu a \sum_{\ell\ell'} \bar{\ell} \gamma^\mu (\sin \theta_{\ell\ell'} - \cos \theta_{\ell\ell'} \gamma_5) \ell' + h.c. \quad (3)$$

Note that $\theta_{\ell\ell'} = 0$ leaves only the parity-even term, while $\theta_{\ell\ell'} = \pi/4$ ($\theta_{\ell\ell'} = 3\pi/4$) is maximally parity-violating, because then the ALP only interacts with left-handed (right-handed) particles.

It is useful to rewrite the leptonic Lagrangian by integrating by parts and solving the classical equations of motion on the leptons. Doing so, we have

$$\mathcal{L}_\ell = \frac{C_{\ell\ell'}}{\Lambda} a \sum_{\ell\ell'} \bar{\ell} (m^- \sin \theta_{\ell\ell'} - m^+ \cos \theta_{\ell\ell'} \gamma_5) \ell' + h.c., \quad (4)$$

where $m^\pm \equiv m_\ell \pm m_{\ell'}$. Here, we note that there is no PV contribution for the flavor-diagonal case, because for $\ell = \ell'$, the difference in masses goes to zero, so we can take $\theta_{\ell\ell} = 0$ without loss of generality. However, there is still parity violation for the off-diagonal couplings. Such a model could lead to an interesting LFV (and potentially parity violating) signal at the EIC. In particular, one can consider the process in Fig. (1), where a can then decay into leptonic final states. We restrict our attention to the τ lepton because of the mass-dependence of the ALP coupling: since $m_\tau \gg m_\mu \gg m_e$, the branching fractions into μ and e final states are negligible. In this scenario, the only terms in the Lagrangian we are interested in are those which contain at least one τ ; in particular,

$$\begin{aligned} \mathcal{L}_\tau &\approx \frac{C_{\tau\ell} m_\tau}{\Lambda} a \sum_{\ell=e,\mu} \bar{\tau} (\sin \theta_{\tau\ell} - \cos \theta_{\tau\ell} \gamma_5) \ell \\ &+ \frac{C_{\tau\tau} m_\tau}{\Lambda} a \bar{\tau} \gamma^5 \tau + h.c., \end{aligned} \quad (5)$$

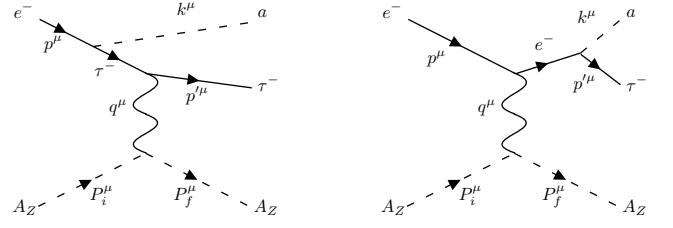


FIG. 1: The diagrams which contribute to the process $eA_Z \rightarrow \tau A_Z a$, where A_Z is the ion nucleus.

where m_e and m_μ are ignored.

CROSS-SECTION CALCULATION

We are now in a position to evaluate the diagram in Fig. (1). The incoming momenta are denoted as p^μ for the electron and P_i^μ for the incoming ion, and the outgoing momenta are denoted as p'^μ for the τ , k for the ALP, and P_f^μ for the outgoing ion. The four-momentum of the exchanged photon is given by $q^\mu \equiv P_i^\mu - P_f^\mu$. For simplicity, we will assume that the ion is a scalar boson with mass M , atomic number Z , and form factor $F(q^2)$, so that the interaction of a photon with the ion is

$$iV^\mu(q^2, P_i, P_f) = ieZF(q^2)(P_i^\mu + P_f^\mu). \quad (6)$$

From here forward, we will specialize to a gold ion ($Z = 79$, mass number $A = 197$), corresponding to a mass of $M = 183$ GeV. The form factor is an approximation of the Fourier transform of the Woods-Saxon distribution applied to the gold nucleus [18], given by

$$F(q^2) = \frac{3}{q^3 R_A^3} (\sin qR_A - qR_A \cos qR_A) \frac{1}{1 + a_0^2 q^2} \quad (7)$$

where $a_0 = 0.79$ fm, $R_A = (1.1 \text{ fm})A^{1/3}$.

For low momentum transfer, $F(q^2) \approx 1$, so the amplitude is proportional to Z . As a result, the cross section will be enhanced by a factor of $79^2 \approx 6000$ for small momentum transfer. This Z^2 enhancement enables the constraints made on $C_{\tau e}$ to be competitive with existing constraints, as we discuss below.

To compute the amplitude, it is useful to define some Mandelstam-like variables in terms of the momenta of the diagram. We have

$$\tilde{s} = (p' + k)^2 - m_e^2 \quad (8)$$

$$\tilde{u} = (p - k)^2 - m_\tau^2 \quad (9)$$

$$t = -q^2 \quad (10)$$

The amplitude calculation is done in full detail in the Appendix; the final spin-averaged result is given by

$$|\overline{\mathcal{M}}|^2 = \left(\frac{4\pi Z \alpha C_{\tau e} m_\tau}{\Lambda} \right)^2 \frac{F(q^2)^2}{q^4} |\overline{\mathcal{A}}|^2, \quad (11)$$

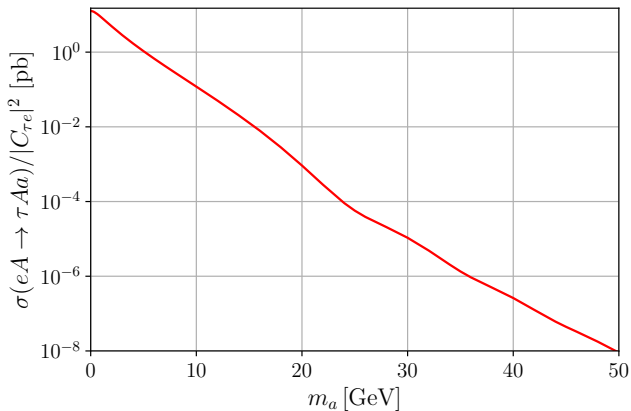


FIG. 2: The cross section for the process $eAZ \rightarrow \tau AZa$ as a function of m_a , assuming an ALP UV scale $\Lambda = 1$ TeV.

where

$$\begin{aligned}
 |\overline{\mathcal{A}}|^2 &= \frac{(\tilde{s} + \tilde{u})^2}{\tilde{s}\tilde{u}} P^2 - 4 \frac{t}{\tilde{s}\tilde{u}} (P \cdot k)^2 \\
 &+ \frac{(\tilde{s} + \tilde{u})^2}{\tilde{s}^2 \tilde{u}^2} (m_a^2 - m_\tau^2 - m_e^2 + 2m_\tau m_e \cos(2\theta_{\tau e})) \\
 &\times \left[P^2 t - 4 \left(\frac{\tilde{u}P \cdot p + \tilde{s}P \cdot p'}{\tilde{s} + \tilde{u}} \right)^2 \right]. \quad (12)
 \end{aligned}$$

Note that for the spin-averaged amplitude, the only dependence on the parity violating angle $\theta_{\tau e}$ is an $\mathcal{O}(m_e/m_\tau)$ correction to the amplitude, so to very good precision one can compute the spin-averaged cross-section with $|\overline{\mathcal{A}}_0|^2 \equiv |\overline{\mathcal{A}}|^2(\theta_{\tau e} = 0)$. We find that these results are in agreement with Refs. [19, 20] with the replacement $m_\tau \rightarrow m_e$ (any apparent sign discrepancies are due to the choice of the metric, which we take to be mostly negative).

To compute the cross section, the integral over phase space is also done following Ref. [20] closely. Defining $x = E_k/|\mathbf{p}|$ to be the fraction of energy the ALP has w.r.t. the electron (assuming $p^0 = |\mathbf{p}|$), the differential cross-section in the rest frame of the ion is given by

$$\frac{d^2\sigma}{dx d\cos\theta_k} = \frac{|\mathbf{k}|}{(32\pi^2)^2 M^2 V} \int_{t_-}^{t_+} dt \int_0^{2\pi} d\phi_q |\overline{\mathcal{M}}|^2, \quad (13)$$

where $V = |\mathbf{V}| = |\mathbf{p} - \mathbf{k}|$, θ_k is the angle \mathbf{k} makes with \mathbf{p} , ϕ_q is the azimuthal angle of \mathbf{q} about \mathbf{V} , and t_\pm are kinematic bounds from the energy-conserving δ -function in the Lorentz-invariant phase space. Details on the phase-space calculation are given in the Appendix.

In order to evaluate the phase-space integral, we must determine the values of the initial-state momenta in Fig. (1). For this, we use Table 10.2 of the EIC Yellow Report [21], which states that the highest energies for the electron and gold ion beams are $|\mathbf{p}^{\text{lab}}| = 18$ GeV and $E_i^{\text{lab}} = 110$ GeV/nucleon, respectively. In the rest frame

of the gold ion, a relativistic calculation reveals that the electron momentum has a magnitude of $|\mathbf{p}| \approx 4200$ GeV.

Next, we must determine the range of integration for $\cos\theta_k$. Following the EIC Yellow Report, we assume a detector pseudorapidity range of $|\eta| < 4$, corresponding to a range of angles $0.04 < \theta^{\text{lab}} < \pi - 0.04$ in the lab frame, or $1.7 \times 10^{-4} \lesssim \theta \lesssim 0.42$ in the rest frame of the ion. We impose the latter limits on the $\cos\theta_k$ integration; in practice, we find that a negligible fraction of events would have θ_k outside of this range. We therefore neglect the detector acceptance of the ALP decay products in terms of their angular directions.

After inserting the kinematic parameters above, the integral can be evaluated. The ϕ_q integrals are computed analytically, but the rest are done numerically. The integrals over t and $\cos\theta_k$ are done using the VEGAS algorithm [22] in Python for a variety of x and m_a , obtaining $d\sigma/dx$ for various m_a . The differential cross section $d\sigma/dx$ can then be integrated over x using the trapezoid rule, obtaining the full cross-section as a function of m_a . The result is shown in Fig. (2).

Finally, we comment on the effect of beam polarization on the ALP signal. To compute the polarized amplitude or cross-section, there are slight modifications to be made. In particular, one can rewrite the τe coupling as

$$\mathcal{L}_{\tau e} \approx \frac{C_{\tau e} m_\tau}{\Lambda} a [R(\theta_{\tau e}) \tau_L^\dagger e_R + L(\theta_{\tau e}) \tau_R^\dagger e_L] + h.c. \quad (14)$$

where $R(\theta) = \cos\theta - \sin\theta$ and $L(\theta) = \cos\theta + \sin\theta$. The left-polarized cross-section can then be obtained by singling out the left-handed piece of Eq. (14). This simply corresponds to setting $\theta_{\tau e} = \pi/4$, then multiplying by $\frac{1}{\sqrt{2}} L(\theta_{\tau e})$. Hence, we find

$$\begin{aligned}
 |\mathcal{A}_L|^2 &= \frac{1}{2} |L(\theta_{\tau e})|^2 |\mathcal{A}(\theta_{\tau e} = \pi/4)|^2 \\
 &\approx |L(\theta_{\tau e})|^2 |\overline{\mathcal{A}}_0|^2, \quad (15)
 \end{aligned}$$

where we have used $|\mathcal{A}(\theta_{\tau e} = \pi/4)|^2 = 2|\overline{\mathcal{A}}(\theta_{\tau e} = \pi/4)|^2 \approx 2|\overline{\mathcal{A}}_0|^2$. The additional factor of 2 accounts for the fact that $|\overline{\mathcal{A}}|^2$ is a spin-averaged quantity. We similarly obtain

$$\begin{aligned}
 |\mathcal{A}_R|^2 &= \frac{1}{2} |R(\theta_{\tau e})|^2 |\mathcal{A}(\theta_{\tau e} = 3\pi/4)|^2 \\
 &\approx |R(\theta_{\tau e})|^2 |\overline{\mathcal{A}}_0|^2. \quad (16)
 \end{aligned}$$

Hence, to good approximation, $\sigma_L = |L(\theta_{\tau e})|^2 \sigma_0$ and $\sigma_R = |R(\theta_{\tau e})|^2 \sigma_0$, where σ_0 represents the spin-averaged cross-section when $\theta_{\tau e} = 0$. This allows us to compute the left-right asymmetry:

$$r_{LR}(\theta_{\tau e}) = \frac{\sigma_L - \sigma_R}{\sigma_L + \sigma_R} = \sin 2\theta_{\tau e} \quad (17)$$

Observation of an ALP signal at varying beam polarizations can thus be used as a direct probe of the parity-violating angle $\theta_{\tau e}$.

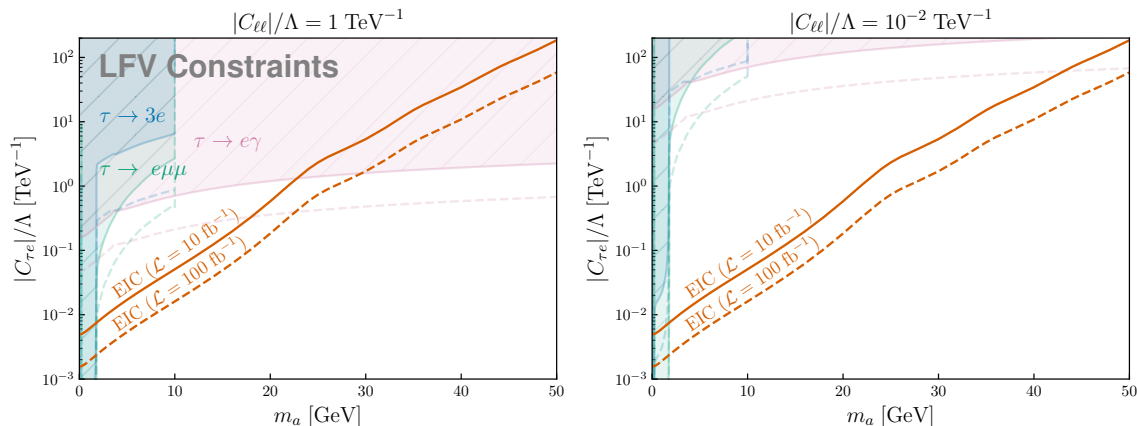


FIG. 3: Projected constraints (95% CL) on the interaction strength $C_{\tau e}$ from the EIC compared to LFV constraints from BABAR (solid lines) and projections from Belle II (dashed lines) for $|C_{\ell\ell}|/\Lambda = 1 \text{ TeV}^{-1}$ (left) and $|C_{\ell\ell}|/\Lambda = 10^{-2} \text{ TeV}^{-1}$ (right). The LFV limits (90% CL) are taken from Ref. [11] for $m_a \leq 10 \text{ GeV}$, while the $\tau \rightarrow e\gamma$ limit is calculated explicitly for $m_a > 10 \text{ GeV}$ with formulae from Ref. [11], since this limit dominates in that regime. The LFV limits in the right panel are scaled up according to their dependence on $|C_{\ell\ell}|/\Lambda$, assuming that any contribution from the $a\gamma\gamma$ coupling is negligible. These results assume that the acceptance times efficiency ϵ is equal to 1.

RESULTS

Once the cross section is determined for a large sample of masses, limits can be placed on the coupling $C_{\tau e}$. Since the process always has an $a e \tau$ vertex, the cross section is proportional to $|C_{\tau e}|^2/\Lambda^2$. As a result, one can write the cross section as

$$\sigma(eA_Z \rightarrow \tau A_Z a) \equiv \frac{|C_{e\tau}|^2}{\Lambda^2} \hat{\sigma}. \quad (18)$$

In what follows, we will assume that the ALP always decays leptonically in the detector, so that we have a $\tau^- \ell^+ \ell'^-$ in the final state. If each lepton is able to be reconstructed, then the final state is clearly LFV unless $\ell = \tau$ and $\ell' = e$, in which case we expect some background. However, even in the most extreme scenario ($C_{\tau\mu} = C_{\tau\tau} = 0$, and the $\tau^- \tau^+ e^-$ state is ignored), this will introduce at most a factor of $\sqrt{2}$ difference in the $C_{\tau e}$ limits. As a result, we will assume zero background for the remainder of the analysis. Then, for a signal acceptance \times efficiency ϵ and an integrated luminosity \mathcal{L} , a value for $C_{\tau e}$ can be ruled out at a 95% C.L. if

$$\frac{|C_{\tau e}|^2}{\Lambda^2} \hat{\sigma} \epsilon \mathcal{L} \leq n_{\text{max}}. \quad (19)$$

where $n_{\text{max}} = 3.09$ is the upper end of the 95% confidence interval for the Poisson signal mean given zero observed signal and background events [23].

As can be seen from the left panel in Fig. (3), for 10 fb^{-1} of integrated luminosity, the EIC is expected to exceed future projections on tau LFV limits for ALP masses larger than m_τ up to $\sim 20 \text{ GeV}$. Increasing the integrated luminosity to 100 fb^{-1} could potentially en-

hance the reach for $C_{\tau e}$ by a factor of ~ 3 , assuming only statistically limited measurements.

Note that we have assumed $\epsilon = 1$, but values below unity will only reduce the sensitivity to $C_{\tau e}$ by $\sqrt{\epsilon}$. Hence, we expect our projections will not be changed significantly with more realistic assumptions for ϵ .

The right panel in Fig. (3) shows the effect of assuming a suppression of the diagonal ALP couplings $C_{\ell\ell}$ by a factor of 100 compared to the left panel, which could be the case in a general framework. In that case, the constraints from τ LFV decays are considerably weakened. However, our EIC production process is only sensitive to $C_{\tau e}$ and would not be affected. Hence, our proposal for exploring this LFV coupling can far exceed future projections using other probes.

CONCLUSIONS

Axion-like particles (ALPs) appear in a wide range of physical settings and may play a role in explaining some of the open questions of particle physics. As such, they are well-motivated subjects of inquiry for theory and experiment. In this work, we considered ALPs, at or above the GeV scale, whose couplings can lead to lepton-flavor-violation (LFV) and may even dominate their interactions with the SM. We focused on $\tau - e$ LFV and showed that the planned electron-ion-collider (EIC) can have considerable reach for this interaction. This is mostly due to two factors: (i) a significant coherent enhancement of low-momentum-transfer electromagnetic scattering from a large Z ion, mediating ALP emission, and (ii) the sizeable center-of-mass energy $\sim 100 \text{ GeV}$ envisioned for the EIC allowing it to reach for ALPs well above the GeV

scale.

The EIC can reach beyond current and projected bounds for $\tau - e$ LFV for ALP masses above m_τ up to $\mathcal{O}(10 \text{ GeV})$, assuming universal diagonal lepton couplings of order $|C_{\ell\ell}|/\Lambda \sim 1 \text{ TeV}^{-1}$. If the diagonal lepton couplings are taken to be smaller, $|C_{\ell\ell}|/\Lambda \sim 10^{-2} \text{ TeV}^{-1}$, then the EIC with $10\text{-}100 \text{ fb}^{-1}$ can exceed projected tau decay search limits for ALP masses up to $\sim 50 \text{ GeV}$. The kinematics of the EIC are particularly favorable for production of ALPs towards the heavier end of this mass range, as opposed to beam dump experiments [20, 24] which benefit from high luminosity and similar Z^2 enhancement, but have much lower collision energy.

One notable observation is that the limits on $C_{\tau e}$ from the EIC are more robust and model-independent than other limits. Although we have focused on LFV constraints, this is generally true. For example, similar constraints were found for a universal all' coupling by analyzing Higgs decays at the LHC in Ref. [6]. These constraints are notably weakened as the ALP-Higgs coupling was decreased, whereas the limits from the EIC would remain unaffected.

We also considered the possibility that ALPs may mediate parity-violating interactions. This, for example, can be realized in certain models with composite ALPs from new strong dynamics. Here, the EIC electron beam polarization can be a powerful probe of such interactions, making it a unique tool for illuminating the physics underlying LFV processes.

In principle, one could consider probing the muon-electron coupling $C_{\mu e}$ at the EIC using a similar search. However, the characteristic mass dependence of ALP couplings reduces the corresponding cross section by $(m_\mu/m_\tau)^2$, so that an EIC search would not typically be competitive with other LFV bounds [11] on $C_{\mu e}$, barring very small lepton-flavor diagonal all and $a\gamma\gamma$ couplings. Production of ALPs via the third LFV coupling $C_{\mu\tau}$ is not accessible in electron-ion collisions, but if both $C_{e\tau}$ and $C_{\mu\tau}$ are significant then $a \rightarrow \mu\tau$ decays could provide access to the latter coupling. Additionally, it may be interesting to consider whether searches at muon beam-dump experiments [25] can give useful bounds on $C_{\mu\tau}$.

Acknowledgements

We thank Nicholas Miesch for helpful discussions in the early stages of this work. This work is supported by

the U.S. Department of Energy under Grant Contracts DE-SC0012704 (H. D.) and DE-SC0010005 (E. N. and R. M.).

-
- [1] R. D. Peccei and H. R. Quinn, Phys. Rev. Lett. **38**, 1440 (1977).
 - [2] S. Weinberg, Phys. Rev. Lett. **40**, 223 (1978).
 - [3] F. Wilczek, Phys. Rev. Lett. **40**, 279 (1978).
 - [4] H. Georgi, D. B. Kaplan, and L. Randall, Phys. Lett. B **169**, 73 (1986).
 - [5] H. Davoudiasl, P. P. Giardino, E. T. Neil, and E. Rinaldi, Phys. Rev. D **96**, 115003 (2017), 1709.01082.
 - [6] H. Davoudiasl, R. Marcarelli, N. Miesch, and E. T. Neil (2021), 2105.05866.
 - [7] M. Gonderinger and M. J. Ramsey-Musolf, JHEP **11**, 045 (2010), [Erratum: JHEP 05, 047 (2012)], 1006.5063.
 - [8] Y. Furtleova and S. Mantry (2021), 2111.03912.
 - [9] Y. Liu and B. Yan (2021), 2112.02477.
 - [10] M. Bauer, M. Neubert, and A. Thamm, JHEP **12**, 044 (2017), 1708.00443.
 - [11] C. Cornella, P. Paradisi, and O. Sumensari, JHEP **01**, 158 (2020), 1911.06279.
 - [12] M. Bauer, M. Neubert, S. Renner, M. Schnubel, and A. Thamm, Phys. Rev. Lett. **124**, 211803 (2020), 1908.00008.
 - [13] M. Bauer, M. Neubert, S. Renner, M. Schnubel, and A. Thamm (2020), 2012.12272.
 - [14] M. Chala, G. Guedes, M. Ramos, and J. Santiago, Eur. Phys. J. C **81**, 181 (2021), 2012.09017.
 - [15] L. Calibbi, D. Redigolo, R. Ziegler, and J. Zupan (2020), 2006.04795.
 - [16] K. Ma (2021), 2104.11162.
 - [17] M. Bauer, M. Neubert, S. Renner, M. Schnubel, and A. Thamm (2021), 2110.10698.
 - [18] S. Klein and J. Nystrand, Phys. Rev. C **60**, 014903 (1999), hep-ph/9902259.
 - [19] Y.-S. Liu, D. McKeen, and G. A. Miller, Phys. Rev. D **95**, 036010 (2017), 1609.06781.
 - [20] Y.-S. Liu and G. A. Miller, Phys. Rev. D **96**, 016004 (2017), 1705.01633.
 - [21] R. Abdul Khalek et al. (2021), 2103.05419.
 - [22] G. P. Lepage, J. Comput. Phys. **439**, 110386 (2021), 2009.05112.
 - [23] G. J. Feldman and R. D. Cousins, Phys. Rev. D **57**, 3873 (1998), physics/9711021.
 - [24] J. D. Bjorken, R. Essig, P. Schuster, and N. Toro, Phys. Rev. D **80**, 075018 (2009), 0906.0580.
 - [25] C.-Y. Chen, M. Pospelov, and Y.-M. Zhong, Phys. Rev. D **95**, 115005 (2017), 1701.07437.

Appendix

Amplitude Calculation

In computing the amplitude, we borrow notation from Refs. [19, 20]. In this appendix, we attempt to provide the amplitude calculation in as much detail as possible, stating explicitly whenever a computer algebra system was used.

Let the incoming four-momenta be p for the electron and P_i for the incoming ion. Let the outgoing momenta be p' for the τ , k for the ALP, and P_f for the outgoing ion. Also, let the mass of the ALP be m_a , the mass of the ion be M , and the charge of the ion be Z . We define $P \equiv P_i + P_f$ and $q \equiv P_i - P_f$, along with the following Mandelstam variables:

$$\tilde{s} = (p' + k)^2 - m_e^2 = 2p' \cdot k + m_a^2 + m_\tau^2 - m_e^2 \quad (\text{A.1})$$

$$\tilde{u} = (p - k)^2 - m_\tau^2 = -2p \cdot k + m_a^2 + m_e^2 - m_\tau^2 \quad (\text{A.2})$$

$$t_2 = (p' - p)^2 = -2p' \cdot p + m_e^2 + m_\tau^2 \quad (\text{A.3})$$

$$t = -q^2, \quad (\text{A.4})$$

which satisfy $\tilde{s} + t_2 + \tilde{u} + t = m_a^2$.

The diagrams in Fig.1 are relatively straightforward, and yield

$$i\mathcal{M}_1 = \bar{u}(p')ie\gamma_\mu \frac{i}{\not{p} - \not{k} - m_\tau} i(\sin\theta_{\tau e} - \gamma_5 \cos\theta_{\tau e}) \frac{m_\tau C_{\tau e}}{\Lambda} u(p) \frac{V^\mu(q^2, P_i, P_f)}{q^2}, \quad (\text{A.5})$$

$$i\mathcal{M}_2 = \bar{u}(p')i(\sin\theta_{\tau e} - \gamma_5 \cos\theta_{\tau e}) \frac{m_\tau C_{\tau e}}{\Lambda} \frac{i}{\not{p}' + \not{k} - m_e} ie\gamma_\mu u(p) \frac{V^\mu(q^2, P_i, P_f)}{q^2}, \quad (\text{A.6})$$

where

$$iV^\mu(q^2, P_i, P_f) = ieZF(q^2)(P_i^\mu + P_f^\mu) \quad (\text{A.7})$$

is the photon-ion interaction vertex. The total amplitude can then be written as

$$i\mathcal{M} = \frac{4\pi Z\alpha C_{\tau e} m_\tau}{\Lambda} \frac{F(q^2)}{q^2} P^\mu \bar{u}(p') \Gamma_\mu(p, k, k') u(p), \quad (\text{A.8})$$

where

$$\Gamma_\mu(p, k, k') = \left[\gamma^\mu \frac{\not{p} - \not{k} + m_\tau}{(p - k)^2 - m_\tau^2} + \frac{\not{p}' + \not{k} - m_e}{(p' + k)^2 - m_e^2} \gamma^\mu \right] \sin\theta_{\tau e} \quad (\text{A.9})$$

$$- \left[\gamma^\mu \frac{\not{p} - \not{k} + m_\tau}{(p - k)^2 - m_\tau^2} - \frac{\not{p}' + \not{k} + m_e}{(p' + k)^2 - m_e^2} \gamma^\mu \right] \gamma_5 \cos\theta_{\tau e}. \quad (\text{A.10})$$

The spin-averaged squared amplitude is then given by

$$|\mathcal{M}|^2 = \left(\frac{4\pi Z\alpha C_{\tau e} m_\tau}{\Lambda} \right)^2 \frac{F(q^2)^2}{q^4} |\overline{\mathcal{A}}|^2, \quad (\text{A.11})$$

with

$$|\overline{\mathcal{A}}|^2 = P^\mu P^\nu \frac{1}{2} \sum_{\sigma\sigma'} \bar{u}_\sigma(p) \Gamma_\mu^\dagger(p, k, k') u_{\sigma'}(p') \bar{u}_{\sigma'}(p') \Gamma_\nu(p, k, k') u_\sigma(p) \quad (\text{A.12})$$

$$= \frac{1}{2} P^\mu P^\nu \text{tr} \{ (\not{p} + m_e) \Gamma_\mu^\dagger(p, k, k') (\not{p}' + m_\tau) \Gamma_\nu(p, k, k') \}. \quad (\text{A.13})$$

One can compute this trace in a computer algebra system, then simplify using the Mandelstam variables defined in Eqs. (A.1-A.4). It is given by

$$|\overline{\mathcal{A}}|^2 = \frac{(\tilde{s} + \tilde{u})^2}{\tilde{s}\tilde{u}} P^2 - 4 \frac{t}{\tilde{s}\tilde{u}} (P \cdot k)^2 + \frac{(\tilde{s} + \tilde{u})^2}{\tilde{s}^2 \tilde{u}^2} M^2(\theta) \left[P^2 t - 4 \left(\frac{\tilde{u}P \cdot p + \tilde{s}P \cdot p'}{\tilde{s} + \tilde{u}} \right)^2 \right], \quad (\text{A.14})$$

where $M^2(\theta) = m_a^2 - m_\tau^2 - m_e^2 + 2m_\tau m_e \cos(2\theta)$. Note that $M^2(\theta) \approx m_a^2 - m_\tau^2$, regardless of θ .

Differential Cross Section Integration

In the initial-state ion rest frame, the differential cross-section is given by

$$d\sigma = \frac{1}{4|\mathbf{p}|M} |\overline{\mathcal{M}}|^2 (2\pi)^4 \delta^4(p' + k - p - q) \frac{d^3\mathbf{p}'}{(2\pi)^3 2E'} \frac{d^3\mathbf{P}_f}{(2\pi)^3 2E_f} \frac{d^3\mathbf{k}}{(2\pi)^3 2E_k}. \quad (\text{A.15})$$

where E' , E_f , and E_k are the time-components of the four-momenta p' , P_f , and k , respectively. The first step in simplifying $d\sigma$ is converting variables from \mathbf{P}_f to \mathbf{q} (which has unit Jacobian) and integrating over \mathbf{p}' . Doing so yields

$$d\sigma = \frac{|\overline{\mathcal{M}}|^2}{1024\pi^5 |\mathbf{p}| M E_f E' E_k} \delta(E' + E_k - E - q_0) d^3\mathbf{q} d^3\mathbf{k} \quad (\text{A.16})$$

In order to simplify some expressions, let $\mathbf{V} = \mathbf{p} - \mathbf{k}$ and $V = |\mathbf{V}|$, and define $\mathbf{q} \equiv (Q, \theta_q, \phi_q)$ in the direction of \mathbf{V} . Then we find

$$E' = \sqrt{Q^2 + V^2 + 2QV \cos \theta_q + m_\tau^2} \quad (\text{A.17})$$

$$E_f = \sqrt{Q^2 + M^2} \quad (\text{A.18})$$

$$E_k = \sqrt{|\mathbf{k}|^2 + m_a^2} \quad (\text{A.19})$$

$$E = \sqrt{|\mathbf{p}|^2 + m_e^2} \quad (\text{A.20})$$

$$q_0 = M - \sqrt{Q^2 + M^2}. \quad (\text{A.21})$$

One can replace E_k systematically with \tilde{u} , since

$$\begin{aligned} \tilde{u} &= (p - k)^2 - m_\tau^2 \\ &= (E - E_k)^2 - |\mathbf{p} - \mathbf{k}|^2 - m_\tau^2 \\ &= (E - E_k)^2 - V^2 - m_\tau^2 \end{aligned} \quad (\text{A.22})$$

$$\implies E_k = E - \sqrt{\tilde{u} + V^2 + m_\tau^2} \quad (\text{A.23})$$

Now we can integrate over θ_q . To do this, note that the argument inside of the delta function

$$f(\cos \theta_q) = E'(\cos \theta_q) + E_k - E - q_0 \quad (\text{A.24})$$

has derivative

$$f'(\cos \theta_q) = \frac{QV}{\sqrt{Q^2 + V^2 + 2QV \cos \theta_q + m_\tau^2}} \quad (\text{A.25})$$

and a zero at

$$\cos \theta_q^0 = \frac{(E - E_k + q_0)^2 - m_\tau^2 - Q^2 - V^2}{2QV}. \quad (\text{A.26})$$

Using this expression for $f'(\cos \theta_q)$ the delta function can be rewritten as

$$\frac{1}{E_f E' E_k} \delta(f(\cos \theta_q)) = \frac{1}{E_f E' E_k} \frac{1}{|f'(\cos \theta_q^0)|} \delta(\cos \theta_q - \cos \theta_q^0) \quad (\text{A.27})$$

$$= \frac{1}{E_k Q V \sqrt{M^2 + Q^2}} \delta(\cos \theta_q - \cos \theta_q^0) \quad (\text{A.28})$$

and the differential cross-section becomes

$$d\sigma = \frac{|\overline{\mathcal{M}}|^2}{1024\pi^5 |\mathbf{p}| M} \frac{1}{E_k Q V \sqrt{M^2 + Q^2}} \delta(\cos \theta_q - \cos \theta_q^0) Q^2 dQ d(\cos \theta_q) d\phi_q d^3\mathbf{k}. \quad (\text{A.29})$$

Note that this solution is not always between -1 and 1 . For $|\cos\theta_q^0| > 1$, the process is kinematically forbidden, and this is enforced by the integral over the δ -function. We can determine when this happens by solving for $\cos\theta_q^0(Q) = \pm 1$, which yields two positive and two negative solutions in Q . We only care about the positive solutions, which yields

$$Q_{\pm} = \left| \frac{V[\tilde{u} + 2(E' + E_f)M] \pm (E' + E_f)\sqrt{\tilde{u}^2 + 4M(E' + E_f)\tilde{u} + 4M^2V^2}}{2(E' + E_f)^2 - 2V^2} \right|. \quad (\text{A.30})$$

As a result, we have

$$d\sigma = \frac{d^3\mathbf{k}}{1024\pi^5|\mathbf{p}|VE_kM} \int_{Q_-}^{Q_+} dQ \frac{Q}{\sqrt{M^2 + Q^2}} d\phi_q \overline{|\mathcal{M}|^2}. \quad (\text{A.31})$$

Alternatively, one can leave the integral over Q unbounded, by noting that the integral of $\delta(\cos\theta_q - \cos\theta_q^0)$ with respect to $\cos\theta_q$ introduces a Heaviside Θ function, which automatically enforces the bounds:

$$d\sigma = \frac{d^3\mathbf{k}}{1024\pi^5|\mathbf{p}|VE_kM} \int_0^\infty dQ \frac{Q}{\sqrt{M^2 + Q^2}} d\phi_q \overline{|\mathcal{M}|^2} \Theta(1 - \cos^2\theta_q^0). \quad (\text{A.32})$$

This is the approach we take when evaluating the integral numerically. To simplify things further, we make a change of variables by introducing the Mandelstam variables t :

$$\begin{aligned} t = -q^2 &= Q^2 - (\sqrt{Q^2 + M^2} - M)^2 \\ &= 2M(\sqrt{M^2 + Q^2} - M). \end{aligned} \quad (\text{A.33})$$

This has $dt/dQ = 2MQ/\sqrt{M^2 + Q^2}$, so

$$d\sigma = \frac{d^3\mathbf{k}}{128\pi^4|\mathbf{p}|VE_k} \int_{t(Q_-)}^{t(Q_+)} dt \left(\frac{1}{8M^2} \int_0^{2\pi} \frac{d\phi_q}{2\pi} \overline{|\mathcal{M}|^2} \right). \quad (\text{A.34})$$

We can now simplify the integral over $d^3\mathbf{k} = |\mathbf{k}|^2 d|\mathbf{k}| d\phi_k d(\cos\theta_k)$ by defining $x = E_k/E$, so that $dx/d|\mathbf{k}| = |\mathbf{k}|/EE_k$. Then,

$$\frac{d\sigma}{dx d(\cos\theta_k)} = \frac{1}{64\pi^3} \frac{|\mathbf{k}|E}{|\mathbf{p}|V} \int_{t(Q_-)}^{t(Q_+)} dt \left(\frac{1}{8M^2} \int_0^{2\pi} \frac{d\phi_q}{2\pi} \overline{|\mathcal{M}|^2} \right) \quad (\text{A.35})$$

$$\approx \frac{1}{64\pi^3} \frac{|\mathbf{k}|}{V} \int_{t(Q_-)}^{t(Q_+)} dt \left(\frac{1}{8M^2} \int_0^{2\pi} \frac{d\phi_q}{2\pi} \overline{|\mathcal{M}|^2} \right) \quad (\text{A.36})$$

where we have taken $m_e \ll |\mathbf{p}|$. It turns out that the integral over ϕ_q can be computed analytically. To do so, one must express the amplitude Eq. (A.14) in terms of the integration variables. We have

$$\mathbf{q} \cdot \mathbf{k} = \frac{Q|\mathbf{k}|}{V} [|\mathbf{p}|(\cos\theta_q^0 \cos\theta_k + \sin\theta_q^0 \sin\theta_k \cos\phi_q) - |\mathbf{k}| \cos\theta_q] \quad (\text{A.37})$$

and

$$\mathbf{q} \cdot \mathbf{p} = \frac{Q|\mathbf{p}|}{V} [|\mathbf{p}| \cos\theta_q^0 - |\mathbf{k}|(\cos\theta_q^0 \cos\theta_k - \sin\theta_q^0 \sin\theta_k \cos\phi_q)]. \quad (\text{A.38})$$

With these, the kinematic terms that appear in Eq. (A.14) can be represented in terms of the integration variables. We have

$$\bar{s} = - \left(1 + \frac{E}{M} \right) t - 2(\mathbf{q} \cdot \mathbf{p}) \quad (\text{A.39})$$

$$\tilde{u} = m_a^2 + m_e^2 - m_\tau^2 - 2xE^2 + 2|\mathbf{p}|\sqrt{x^2E^2 - m_a^2} \cos\theta_k \quad (\text{A.40})$$

$$P^2 = 4M^2 + t \quad (\text{A.41})$$

$$P \cdot k = \left(2M + \frac{t}{2M} \right) xE + \mathbf{q} \cdot \mathbf{k} \quad (\text{A.42})$$

$$P \cdot p = \left(2M + \frac{t}{2M} \right) E + \mathbf{q} \cdot \mathbf{p} \quad (\text{A.43})$$

$$P \cdot p' = P \cdot p - P \cdot k. \quad (\text{A.44})$$

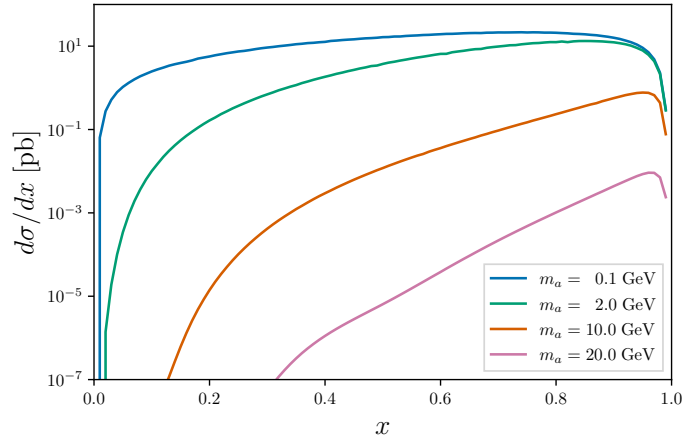


FIG. 4: The differential cross section for the process $eA_Z \rightarrow \tau A_Z a$ as a function of the energy fraction $x = E_k/p$ for $m_a = 0.1, 2.0, 10.0,$ and 20.0 GeV, assuming an interaction strength $|C_{\tau e}|/\Lambda = 1 \text{ TeV}^{-1}$.

To compute the integral over ϕ_q , we note that the only place ϕ_q appears is in the $\cos \phi_q$ inside of $\mathbf{q} \cdot \mathbf{k}$ and $\mathbf{q} \cdot \mathbf{p}$. As a result, each of the terms in Eq. (A.14) can be written in the form

$$A + \frac{B}{C + D \cos \phi_q} + \frac{E}{(C + D \cos \phi_q)^2}. \quad (\text{A.45})$$

This can then be integrated over ϕ_q to obtain

$$\int_0^{2\pi} \frac{d\phi_q}{2\pi} \left[A + \frac{B}{C + D \cos \phi_q} + \frac{E}{(C + D \cos \phi_q)^2} \right] = A + \frac{B}{(C^2 - D^2)^{1/2}} + \frac{CE}{(C^2 - D^2)^{3/2}} \quad (\text{A.46})$$

so in principle, $\int_0^{2\pi} \frac{d\phi_q}{2\pi} |\overline{\mathcal{A}}|^2$ can be computed analytically. The constants $A, B, C, D,$ and E are complicated functions of the kinematic variables and differ term-by-term, so we do not write them out explicitly. However, this substitution can be made in a computer algebra system so that the only remaining integrals are over $t, \cos \theta_k,$ and x . Those integrals can then be computed numerically. The results of integrating over t and $\cos \theta_k$ for a range of m_a are shown in Fig. 4.